Biosensors and Bioelectronics 153 (2020) 112045

Contents lists available at ScienceDirect

Biosensors and Bioelectronics

journal homepage: http://www.elsevier.com/locate/bios

Electrochemical dopamine sensor based on superionic conducting potassium ferrite

Xuejiao Sun [a], Le Zhang [a], Xinghui Zhang [a], Xinxin Liu [b], Juan Jian [c], Dechen Kong [a], Decheng Zeng [a], Hongming Yuan [a,*], Shouhua Feng [a]

[a] State Key Laboratory of Inorganic Synthesis and Preparative Chemistry, College of Chemistry, Jilin University, Changchun, 130012, PR China
[b] Institute of Catalysis for Energy and Environment, College of Chemistry and Chemical Engineering, Shenyang Normal University, Shenyang, 110034, China
[c] Key Laboratory of Functional Materials Physics and Chemistry of the Ministry of Education, College of Chemistry, Jilin Normal University, Siping, 136000, PR China

ARTICLE INFO

Keywords:
Potassium ferrite
Ionic conductor
Modified electrode
Dopamine
Electrochemical biosensor

ABSTRACT

Ionic liquid composite electrodes have been widely utilized for the fabrication of electrochemical biosensors. However, the biosensing electrode modified with ionic conducting solids remains unexplored. Herein, we prepared a superionic conducting potassium ferrite ($K_2Fe_4O_7$) under hydrothermal conditions for modifying glassy carbon electrode (GCE). The modified electrode ($K_2Fe_4O_7$/GCE) showed an excellent electrocatalytic activity towards the oxidation of dopamine (DA). The oxidation peak currents increased linearly with increasing DA concentrations in the range of 1 μM–140 μM, and the detection limit is 0.22 μM (S/N = 3). The developed DA sensor exhibited not only good selectivity for the determination of DA without interfering from ascorbic acid (AA), uric acid (UA), glucose and inorganic ions, but also good reproducibility and stability. Furthermore, the sensor was applied to determine DA concentration in bovine serum and obtained a satisfied result. This study provides a new approach for developing electrochemical biosensors based on ionic conducting solid materials.

1. Introduction

Dopamine (DA) is a crucial neurotransmitter that effects on many systems in body including cardiovascular, renal, and hormonal functioning (Freeman et al., 2007). Diverse neurological diseases can result from disruptions of the dopaminergic neuron process (Hirsch et al., 1988; Oh et al., 2016; Tang et al., 2007). The importance of dopamine cannot be overstated in the diagnosis of neurological disorders (Laviolette, 2007). Hence, the DA detection in biological system is paramount in routine monitoring purposes.

To detect DA concentration, several quantitative analytical techniques have been developed. Among them, electrochemical biosensors present numerous advantages over high performance liquid chromatography (HPLC) (Hows et al., 2004) and mass spectroscopy (Huang et al., 2014a), including low cost, portability, simple operation, and fast detection (Huang et al., 2018; Guo, 2017; Guo et al., 2018; Xu et al., 2018a,c). The conventional electrochemical biosensors for the detection of DA are usually fabricated by using GCE or carbon electrodes. However, such electrodes exhibited some limitations in terms of electron transfer ability, sensitivity, and selectivity. Subsequently, a major strategy for enhancing DA sensor performance is using chemical-modified electrodes with electrical conducting materials to accelerate electrochemical reaction at the interface (Beitollahia et al., 2019). Up to now, many electronic conducting or semiconducting materials, including organic molecules (Lai et al., 2007; Shervedani et al., 2006; Uzun and Hasdemir, 2017), polymers (Chen et al., 2010; Song et al., 2010; Xu et al., 2018b), metals or metal alloy (Hsu et al., 2012; Yu et al., 2012; Yusoff et al., 2015; Zhao et al., 2016), carbon materials, (Gao et al., 2013; Huang et al., 2014b; Kim et al., 2010; Ku et al., 2013; Liu et al., 2012; Palanisamy et al., 2013; Qi et al., 2015; Rajkumar et al., 2017; Yang et al., 2019; Yuan et al., 2012) and metal oxides, (Adekunle et al., 2010; Anithaa et al., 2015; Fan et al., 2011; Liu et al., 2013; Zhang et al., 2008) have been used to modify the bare electrodes, resulting in increasing the performance of electrochemical DA sensors.

Ionic liquids (ILs) consisting of ions are intrinsically ionic conductors. Over the past decade, there has been growing interest in the fabrication and application of IL-based electrochemical biosensors because of their unique physical and chemical properties, such as good ionic conductivity, wide potential windows and biocompatibility (Cheng et al., 2018; Shiddiky and Torriero, 2011). In particular, a

* Corresponding author.
E-mail address: hmyuan@jlu.edu.cn (H. Yuan).

https://doi.org/10.1016/j.bios.2020.112045
Received 6 November 2019; Received in revised form 13 January 2020; Accepted 20 January 2020
Available online 21 January 2020

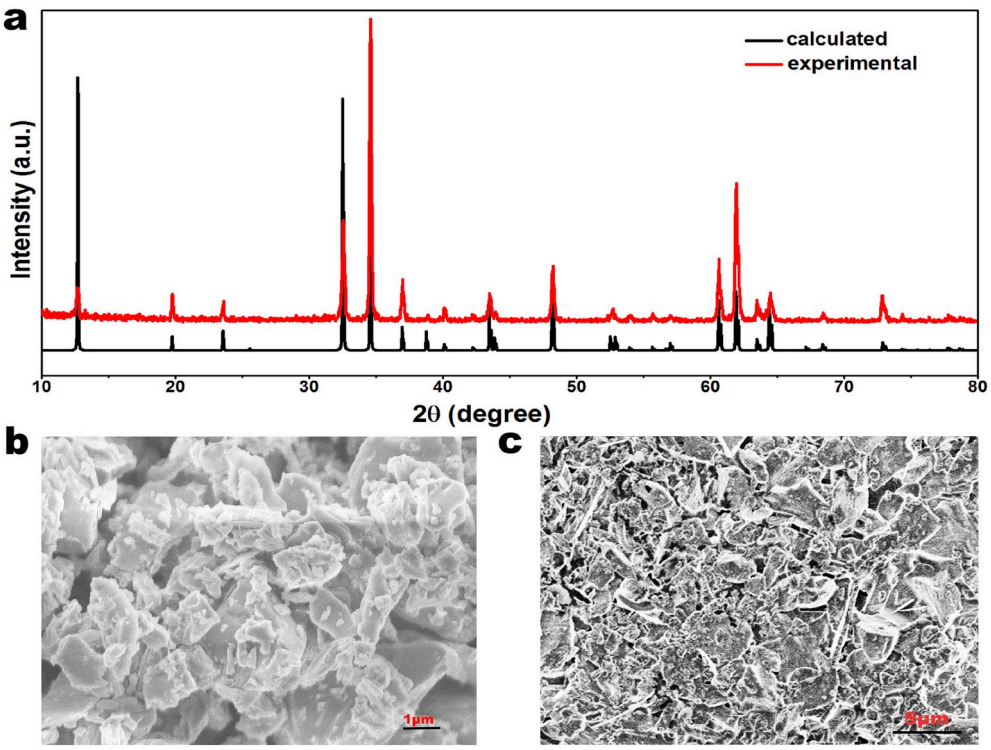

Fig. 1. **(a)** The calculated and powder XRD patterns of $K_2Fe_4O_7$. The SEM images of **(b)** $K_2Fe_4O_7$ particles after ball-milling and **(c)** $K_2Fe_4O_7$ layer attached on the surface of GCE.

carbon electrode modified with *n*-octylpyridinum hexafluorophosphate (IL) has been applied for the determination of DA (Safavi et al., 2006). A 1-butyl-3-methylimidazolium hexafluorophosphate (IL) and carbon nanotube composite material-modified electrode has showed better selectivity in detecting DA (Wang et al., 2015; Zhang et al., 2008). Clearly, the modification of carbon electrodes with different ILs promoted electrical conductivity of modified electrodes through the synergistic effect. However, there still are many obstacles related to the achievement of highly stable and reliable IL-based electrochemical DA sensors, since ILs can easily absorb water and react with it and are prepared difficultly.

Ionic conducting solid materials have been widely used in electrocatalysis, electrochemical capacitors, and rechargeable batteries (Jesús et al., 2015; Qiu et al., 2019). An electrochemical sensor for the detection of lithium ions in authentic human saliva has been fabricated by using the modified GCE with mixed ion/electron conducting $LiMn_2O_4$ (Suherman et al., 2019). The use of modified electrodes with ionic conducting solid electrolytes may provide high performance DA sensor but with significantly lower cost and fabricating requirements. Nevertheless, so far there has been no report on such materials used as an electrode modifier for DA detection. More recently, we have reported the hydrothermal synthesis of superionic conducting potassium ferrite (Yuan et al., 2018). This environmentally friendly iron oxide demonstrated superhigh ionic conductivity and excellent thermal and electrochemical stability.

In this work, we firstly prepared potassium ferrite by hydrothermal technique. A modified GCE with this superionic conductor was proposed, and then the modified electrode ($K_2Fe_4O_7$/GCE) was used as working electrode of DA sensor for the sensitive and selective detection of DA in the coexistence of AA, UA, glucose, and inorganic ions. We also carried out evaluating reproducibility and stability of the obtained DA sensor. Furthermore, the sensor was applied to detect DA concentration in bovine serum.

2. Materials and methods

2.1. Reagents and chemicals

Dopamine, uric acid (AA) and ascorbic acid (UA) were purchased from Sigma-Aldrich (Shanghai, China). $Fe(NO_3)_3{\cdot}9H_2O$, KOH, KH_2PO_4, K_2HPO_4, $K_3Fe(CN)_6$, $K_4Fe(CN)_6$, KCl, NaCl and glucose were purchased from Sinopharm Chemical Reagent. Co. (China). The bovine serum was purchased from Solarbio. Co. (China). All chemicals were of analytical grade and used without any treatment. The phosphate buffer solution (PBS, 0.1 M) as supporting electrolyte was prepared with K_2HPO_4 and KH_2PO_4, and the pH value ranging from 7.0 to 7.8 was adjusted by changing the radio of K_2HPO_4 and KH_2PO_4. Aqueous solutions used in experiments were prepared using deionized water with resistance 5 MΩ-cm obtained from an ultrapure water system (Wotepu, China). All solutions were freshly prepared every day, and were purged with N_2 for 30 min before used in the electrochemical experiment.

2.2. Instruments and measurements

Powder X-ray diffraction (PXRD) experiments were measured on a Rigaku D-Max 2550 diffractometer (Rigaku, Japan) with Cu-Kα radiation ($\lambda = 1.5418$ Å). The scanning electron microscope (SEM) images were obtained on a JEOL-6700 scanning electron microscope (Tokyo, Japan). UV–Vis absorption spectra were collected within wavelength range of 350–600 nm with a UV-2450 spectrometer (Hitachi, Japan). All electrochemical measurements were carried out at room temperature by using a CHI660C electrochemical workstation (Chenhua Co., Shanghai, China). Electrochemical impedance spectroscopy (EIS), cyclic voltammetry (CV), differential pulse voltammetry (DPV) and Chronoamperometry (i-t curve) were performed in a conventional three-electrode cell consisting of a bare or modified GCE as working electrode, Ag/AgCl/KCl (0.1 M) as the reference electrode, platinum as the counter electrode.

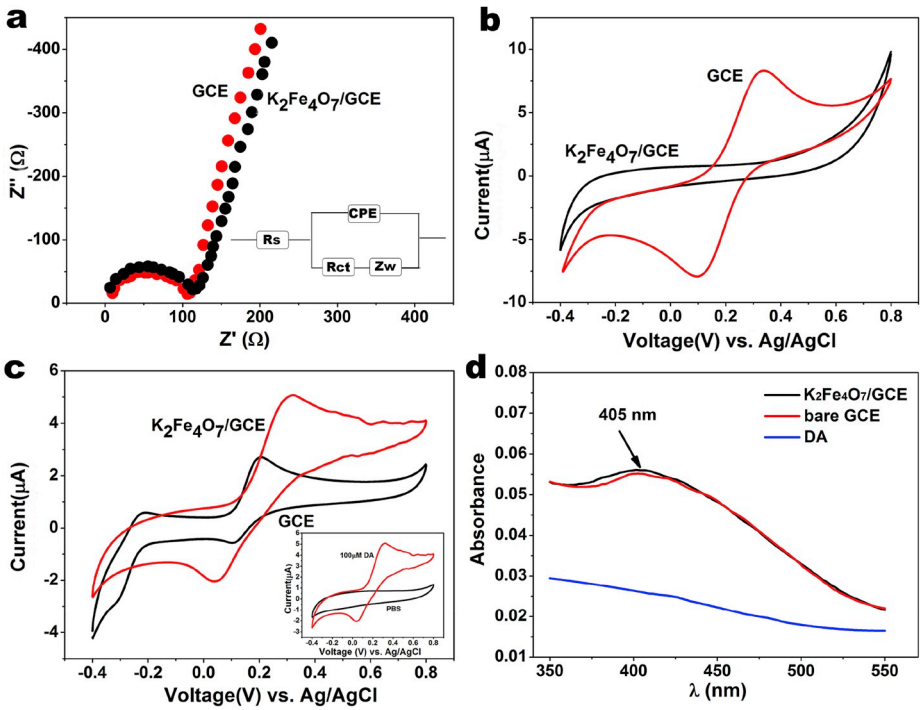

Fig. 2. **(a)** Nyquist plots and **(b)** CVs of bare GCE and $K_2Fe_4O_7$/GCE in 0.1 M KCl containing 1 mM $Fe(CN)_6^{3-/4-}$. The EIS are measured in the frequency region from 1 MHz to 1 Hz. Inset displays the equivalent circuit. **(c)** CVs of bare GCE and $K_2Fe_4O_7$/GCE in 0.1 M PBS (pH = 7.6) containing 100 μM DA. Inset shows the CVs of $K_2Fe_4O_7$/GCE in the absence and presence of 100 μM DA. **(d)** The UV–Vis absorption spectra of 100 μM DA in 0.1 M PBS (pH = 7.6) before and after applying voltage of 0.8 V at bare GCE and $K_2Fe_4O_7$/GCE.

2.3. Preparation of $K_2Fe_4O_7$ powder and fabrication of $K_2Fe_4O_7$-modified electrode

By using the same hydrothermal process reported by us previously (Yuan et al., 2018), single crystal of $K_2Fe_4O_7$ was obtained, and then obtained crystal was grounded into powder by ball milling treatment.

2.4. Fabrication of $K_2Fe_4O_7$-modified GCE

A GCE (diameter = 3 mm) was polished with 0.05 μm alumina slurry. After ultrasonic cleaning in deionized water for 2 min, the electrode was dried in air at ambient temperature. The dispersion of $K_2Fe_4O_7$ was prepared by adding as-prepared $K_2Fe_4O_7$ powder of 5 mg to a mixture of 5 mL Dimethyl Formamide and 1 μL Nafion followed by ultrasonication for 30 min. Subsequently, the dispersion was drop-cast onto the GCE surface and dried in air at ambient temperature overnight. A stable $K_2Fe_4O_7$ layer has been immobilized on the GCE surface.

3. Results and discussion

3.1. Characterization of $K_2Fe_4O_7$ powder and layer

The X-ray diffraction technique is employed to identify the crystalline phase and purity. As shown in Fig. 1a, the PXRD pattern of the sample obtained by ball-milling are in accordance with the pattern that was simulated on the basis of the single-crystal structure (Yuan et al., 2018), indicating that its crystal structure is well remained and the sample has not impure phase. SEM was used to observe surface morphology of $K_2Fe_4O_7$ particle and layer. The SEM image (Fig. 1b) shows that particle sizes are different and less than 3 μm in side length. A uniform $K_2Fe_4O_7$ layer was closely attached on the surface of GCE (Fig. 1c).

3.2. Characterization of $K_2Fe_4O_7$/GCE electrode

The electrochemical behavior of bare GCE and $K_2Fe_4O_7$/GCE electrodes are investigated by EIS and CV. Fig. 2a showed Nyquist plots for bare GCE and $K_2Fe_4O_7$/GCE in 0.1 M KCl containing 1 mM $K_3Fe(CN)_6$ and 1 mM $K_4Fe(CN)_6$. A standard Randle's equivalent circuit model was used to fit the impedance data (insert in Fig. 2a), where R_s, CPE, R_{ct}, and Z_w represent the uncompensated solution resistance, a constant phase element, charge transfer resistance and Warburgh impedance, respectively (Huang et al., 2013). Two electrodes exhibited R_{ct} values of 107 Ω and 115 Ω, indicating that the electrical conductivity of bare GCE is very close to that of the modified electrode. As is well-known, $Fe(CN)_6^{3-/4-}$ as redox probes involve only in single electron transfer process. To determine the nature of the transfer charges, the CV measurements were carried out in $Fe(CN)_6^{3-/4-}$ solutions. As shown in Fig. 2b, for the bare GCE, a pair of typical redox peaks of $Fe(CN)_6^{3-/4-}$ ion was recorded, which is consistent with the literature result (Qi et al., 2015). However, under the same conditions, no peaks were observed for $K_2Fe_4O_7$/GCE electrode since $K_2Fe_4O_7$ is a superionic conductor and inhibited the electron-transfer of $Fe(CN)_6^{3-/4-}$. Therefore, at $K_2Fe_4O_7$/GCE electrode, the transfer charge is ionic.

3.3. Electrocatalytic oxidation of DA at $K_2Fe_4O_7$/GCE electrode

Not only does the redox reaction of DA involve in losing and gaining two electrons, but also in losing and gaining two protons. Fig. 2c shows the CV responses of 100 μM DA in 0.1 M PBS (pH = 7.6) at bare GCE and $K_2Fe_4O_7$/GCE. For bare GCE, two pairs of redox peaks were observed. The peaks at 0.192 V (anodic) and 0.124 V (cathodic) are attributed to the redox reaction between DA and dopaminequinone (DAQ). The remaining peaks at −0.201 V and −0.282 V come from the oxidation of DAQ to leucodopaminochrome (LDAC) and the reduction of LDAC back to DAQ (Hawley et al., 1966; Wang et al., 2006). However, for $K_2Fe_4O_7$/GCE, the CV curve exhibited only a well-defined pair of redox peaks with potentials of 0.323 V and 0.042 V, suggesting that DA was oxidized only to DAQ. To further confirm the oxidation of DA to DAQ, the UV–Vis absorption technique is used to detect the generation of DAQ. As shown in Fig. 2d, no absorption peak was observed for 100 μM DA in PBS. After applying voltage of 0.8 V to the bare GCE and $K_2Fe_4O_7$/GCE electrodes for 30 min, the characteristic absorption peak appeared at 405 nm corresponding to DAQ (Bisaglia et al., 2010). The inset in Fig. 2c gives the CV curves recorded in the presence and absence of 100 μM DA at $K_2Fe_4O_7$/GCE in 0.1 M PBS (pH = 7.6) at the scan rate

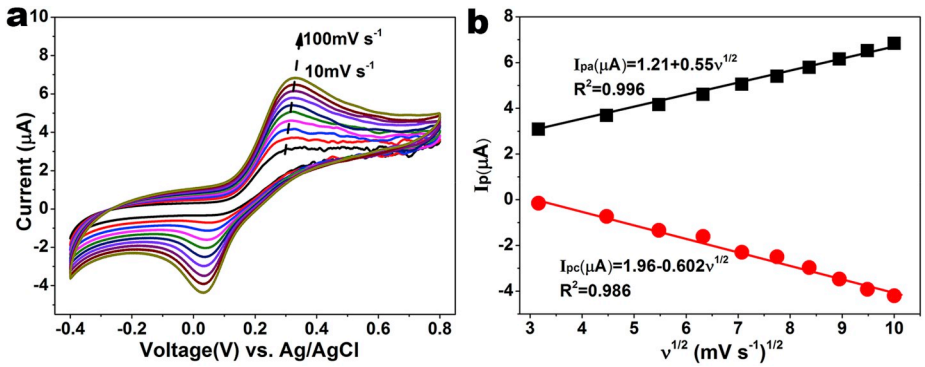

Fig. 3. **(a)** CVs of $K_2Fe_4O_7$/GCE in 0.1 M PBS (pH = 7.6) containing 100 μM DA at scan rates of 10–100 mV s^{-1}. **(b)** The plots of redox peak currents as a function of scan rate.

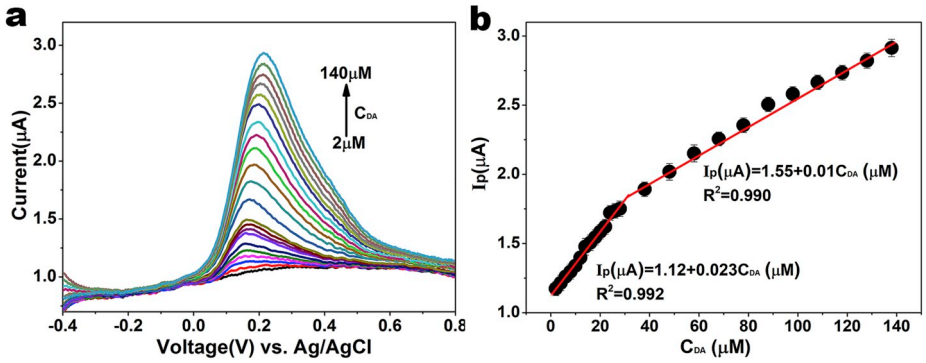

Fig. 4. **(a)** DPV records of $K_2Fe_4O_7$/GCE for different DA concentrations in 0.1 M PBS (pH = 7.6). **(b)** Plots of the oxidation peak current *vs.* DA concentrations (1–140 μM).

of 50 mV s^{-1}. Since there was no CV response in DA-free solution, it can be concluded that the charge transfer between DA and ionic conducting $K_2Fe_4O_7$ is achieved through ionic diffusion. In addition, the corresponding redox currents obtained at the modified electrode was two times that at the bare GCE (Fig. 2c), indicating a faster ionic transfer rate for the oxidation of DA at $K_2Fe_4O_7$/GCE.

3.4. The effect of pH value and scan rate

The effect of pH value in the electrolyte solution on the response current of DA was examined in the range of pH = 7.0 to 7.8. As depicted in Fig. S1, the response current increased linearly with increasing pH value to 7.6 and then it decreased at higher pH value. Thus, pH = 7.6 was an optimal value for further experiments.

The effect of scan rate on electrochemical reaction of DA at $K_2Fe_4O_7$/GCE was investigated by CV. Fig. 3a shows the CVs of $K_2Fe_4O_7$/GCE electrode in PBS (pH = 7.6) containing 100 μM DA at various scan rates (10–100 mV s^{-1}). With increasing scan rate, the oxidation and reduction currents (Ipa and Ipc) increase and simultaneously the anodic peak potential shifted positively and negatively for the cathodic peak potential. Moreover, the ratio of Ipa to Ipc was 2.5. These results suggest that the electrochemical oxidation and reduction of DA is a quasi-reversible behavior (Adekunle et al., 2010; Anithaa et al., 2015). Ipa and Ipc as function of the square root of scan rates ($\nu^{1/2}$) are plotted in Fig. 3b. Two linear regression equations, Ipa(μA) = $0.55\nu^{1/2} + 1.21$ ($R^2 = 0.994$) and Ipc(μA) = $1.958–0.602\nu^{1/2}$ ($R^2 = 0.986$), were obtained, inferring that the electrochemical reaction is a typical diffusion-controlled process (Majdi et al., 2007; Wang et al., 2007).

Table 1
Comparison of the fabricated DA sensors reported in the literatures.

Electrode	Linear Range (μM)	Detection Limit (μM)	Ref
PEDOT-LSG	1–150	0.33	Xu et al. (2018b)
RGO-Pd-NPs	1–150	0.233	Palanisamy et al. (2013)
CC-NPC	2–200	0.6	Zhao et al. (2016)
Graphene-GCE	4–100	2.64	Kim et al. (2010)
Go-GCE	1–15	0.27	Gao et al. (2013)
MIPs-pThi-NPG	0.3–100	0.1	Yang et al. (2019)
SWCNTs-GCE	0.5–100	0.19	Yang et al. (2019)
WO_3-GCE	0.1–50, 50-600	0.024	Anithaa et al. (2015)
TiO_2-graphene-GCE	5–200	2	Fan et al. (2011)
CoHCF-GCE	300–5000	1	Xun et al. (2003)
$K_2Fe_4O_7$ -GCE	1-40, 40-140	0.22	this work

3.5. Calibration curve

The oxidation peak current of DA was selected as a signal relative to the concentration of DA. Fig. 4a displays DPV responses of the modified electrode at different DA concentrations in 0.1 M PBS at pH = 7.6. The corresponding plots of peak currents and DA concentrations are shown in Fig. 4b. It could be seen that the linear relationship between them was obtained in the concentration range of 1–140 μM. For DA concentrations (C_{DA}) ranging from 1 to 40 μM, the linear regression equation is Ip(μA) = $1.12 + 0.023C_{DA}$ (μM) ($R^2 = 0.992$), and Ip(μA) = $1.55 + 0.01C_{DA}$ (μM) ($R^2 = 0.990$) from 40 to 140 μM. The detection limit is calculated to be 0.22 μM based on the signal corresponding to three times noise of the response (S/N = 3). Compared with other published works (seen in Table 1), the low detection limit and wide linear range of the prepared

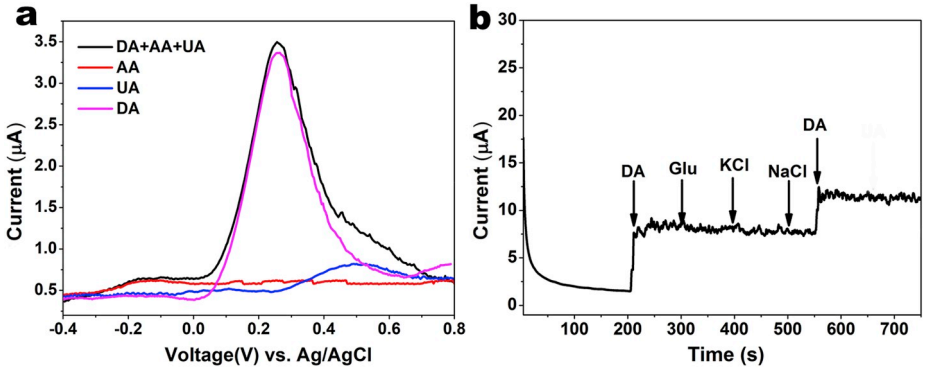

Fig. 5. **(a)** DPV responses of $K_2Fe_4O_7$/GCE in 0.1 M PBS (pH = 7.6) for 1 mM AA, 100 μM DA, 100 μM UA and the mixture of 1 mM AA, 100 μM DA and100 μM UA. **(b)** Amperometric responses of the $K_2Fe_4O_7$/GCE for the addition of 200 μM DA and 200 μM glucose, 200 μM KCl and 200 μM NaCl in 0.1 M PBS (pH = 7.6).

sensor make it practical for device application.

3.6. Selectivity of the sensor

AA, UA, glucose, KCl and NaCl are well-known interfering species in the electrochemical detection of DA in biological samples (Fu et al., 2019; Guo, 2016a; Guo and Ma, 2017). The selectivity of the $K_2Fe_4O_7$/GCE electrode to DA was evaluated by recording its DPV response to abovementioned interfering AA and UA molecules. Fig. 5a shows DPV curve recorded in PBS (pH = 7.6) for 1 mM AA, 100 μM DA, 100 μM UA and the mixture of these compounds. Obviously, the peak current towards DA was much higher than that towards AA and UA. The high specificity is due to the oxidation products of AA and UA being electro-inactive (Zen et al., 2004). In the presence of other interfering substances, the selectivity of the $K_2Fe_4O_7$/GCE electrode to DA was evaluated by Chronoamperometry method (Fig. 5b). No response current changes of glucose, KCl and NaCl were observed after adding 200 μM glucose, 200 μM KCl and 200 μM NaCl. A large current change was detected at a DA concentration of 200 μM, indicating that the sensor presents a high selectivity to DA molecules.

3.7. Reproducibility and stability of the sensor

The reproducibility of the sensor was examined by detecting the DPV response of 100 μM DA in PBS (pH = 7.6) with the same electrode eight times. The detecting results are shown in Fig. S2a. The relative standard deviation (RSD) was about 1.07%. Under the same condition, the five electrodes exhibit an RSD of 0.16%, showing good reproducibility (Fig. S2b). When not used, the sensor was stored in PBS at 4 °C. The DPV responses of 100 μM DA in PBS (pH = 7.6) were measured every day (Fig. S2c). The sensor retained a response current of 93.1% of its initial current after 5 days.

3.8. Determination of DA in bovine serum

The serum is the most normal matrix for the sensors to apply (Fu and Guo, 2018; Guo, 2016b; Wang et al., 2018). To evaluate the accuracy and applicability of the fabricated sensor, it was employed to determine DA concentration in bovine serum samples. The serum samples were diluted 100 times using 0.1 M PBS before determination. The experiment was performed using five samples with different DA concentration. The analytical results are listed in Table S1. The measured concentrations are close to the labeled values, and the RSD values were below 2.63%.

4. Conclusions

A novel electrochemical DA sensor was successfully constructed by using the modified electrode with potassium ferrite. The modified electrode has good charge-transfer ability and shows an excellent electrocatalytic activity towards DA. The developed DA sensor with good linear range and low detection limit demonstrates excellent selectivity and reproducibility, as well as stability and is a potential biosensor for DA detection in biological system. In the future, its sensing performance could be improved by compositing with electron conducting materials.

Declaration of competing interest

The authors declare that they have no known competing financial interests or personal relationships that could have appeared to influence the work reported in this paper.

CRediT authorship contribution statement

Xuejiao Sun: Conceptualization, Methodology, Software, Investigation, Data curation, Writing - original draft, Writing - review & editing. **Le Zhang:** Validation, Formal analysis, Visualization, Software. **Xinghui Zhang:** Validation, Formal analysis, Visualization. **Xinxin Liu:** Writing - review & editing. **Juan Jian:** Writing - review & editing. **Dechen Kong:** Writing - review & editing. **Decheng Zeng:** Writing - review & editing. **Hongming Yuan:** Resources, Writing - review & editing, Supervision, Data curation. **Shouhua Feng:** Writing - review & editing.

Acknowledgements

This work is supported financially by State Key Laboratory of Inorganic Synthesis and Preparative Chemistry.

Appendix A. Supplementary data

Supplementary data to this article can be found online at https://doi.org/10.1016/j.bios.2020.112045.

References

Adekunle, A., Agboola, B., Pillay, J., Ozoemena, K., 2010. Electrocatalytic detection of dopamine at single-walled carbon nanotubes-iron (III) oxide nanoparticles platform. Sensor. Actuator. B Chem. 148, 93–102.

Anithaa, A., Lavanya, N., Asokan, K., Sekar, C., 2015. WO_3 nanoparticles based direct electrochemical dopamine sensor in the presence of ascorbic acid. Electrochim. Acta 167, 294–302.

Beitollahia, H., Safaeia, M., Tajik, S., 2019. Different electrochemical sensors for determination of dopamine as neurotransmitter in mixed and clinical samples: a review. Anal. Bioanal. Chem. Res. 6, 81–96.

Bisaglia, M., Soriano, M., Arduini, I., Mammi, S., Bubacco, L., 2010. Molecular characterization of dopamine-derived quinones reactivity toward NADH and glutathione: implications for mitochondrial dysfunction in Parkinson disease. Biochim. Biophys. Acta 1802, 699–706.

Chen, R., Ratnikova, T., Stone, M., Lin, S., Lard, M., Huang, G., Hudson, J., Ke, P., 2010. Differential uptake of carbon nanoparticles by plant and mammalian cells. Small 6, 612–617.
Cheng, H., Hu, C., Ji, Z., Ma, W., Wang, H., 2018. A solid ionic Lactate biosensor using doped graphene-like membrane of Au-EVIMC-titania nanotubes-polyaniline. Biosens. Bioelectron. 118, 97–101.
Fan, Y., Lu, H., Liu, J., Yang, C., Jing, Q., Zhang, Y., Yang, X., Huang, K., 2011. Hydrothermal preparation and electrochemical sensing properties of TiO_2-graphene nanocomposite. Colloids Surf., B 83, 78–82.
Freeman, R., Elbaz, J., Gill, R., Zayats, M., Willner, I., 2007. Analysis of dopamine and tyrosinase activity on ion-sensitive field-effect transistor (ISFET) devices. Chem. Eur J. 13, 7288–7293.
Fu, Y., Guo, J., 2018. Blood cholesterol monitoring with smart phone as miniaturized electrochemical analyzer for cardiovascular disease prevention. IEEE Trans. Biomed. Circ. Syst. 12, 784–790.
Fu, Y., Yang, H., Guo, J., 2019. Electrochemical test strip-based accurate blood uric acid measurement by adding blood cell filtration membrane. IEEE Trans. Biomed. Circ. Syst. 15, 6389–6394.
Gao, F., Cai, X., Wang, X., Gao, C., Liu, S., Gao, F., Wang, Q., 2013. Highly sensitive and selective detection of dopamine in the presence of ascorbic acid at graphene oxide modified electrode. Sensor. Actuator. B Chem. 186, 380–387.
Guo, J., 2016a. Uric acid monitoring with a smartphone as the electrochemical analyzer. Anal. Chem. 88, 11986–11989.
Guo, J., 2016b. Smartphone-powered electrochemical dongle for point-of-care monitoring of blood β-ketone. Anal. Chem. 89, 8609–8613.
Guo, J., 2017. Smartphone-powered electrochemical biosensing dongle for emerging medical IoTs application. IEEE Trans. Biomed. Circ. Syst. 14, 2592–2597.
Guo, J., Huang, X., Ma, X., 2018. Clinical identification of diabetic ketosis/diabetic ketoacidosis acid by electrochemical dual channel test strip with medical smartphone. Sensor. Actuator. B Chem. 275, 446–450.
Guo, J., Ma, X., 2017. Simultaneous monitoring of glucose and uric acid on a single test strip with dual channels. Biosens. Bioelectron. 94, 415–419.
Hawley, M., Tatawawadi, S., Piekarski, S., Adams, R., 1966. Electrochemical studies of the oxidation pathways of catecholamines. J. Am. Chem. Soc. 89, 447–450.
Hsu, H., Chen, Y., Lee, C., Chiu, H., 2012. Gold nanostructures on flexible substrates as electrochemical dopamine sensors. ACS Appl. Mater. Interfaces 4, 5570–5575.
Hirsch, E., Graybielt, A.M., Agid, Y.A., 1988. Melanized dopaminergic neurons are differentially susceptible to degeneration in Parkinson's disease. Nature 334, 345–348.
Hows, M., Lacroix, L., Heidbreder, C., Organ, A., Shah, A., 2004. High-performance liquid chromatography/tandem mass spectrometric assay for the simultaneous measurement of dopamine, norepinephrine, 5-hydroxytryptamine and cocaine in biological samples. J. Neurosci. Methods 138, 123–132.
Huang, Y., Cheng, C., Tian, X., Zheng, B., Li, Y., Yuan, H., Xiao, D., Choi, M., 2013. Low-potential amperometric detection of dopamine based on MnO_2 nanowires/chitosan modified gold electrode. Electrochim. Acta 89, 832–839.
Huang, F., Li, J., Shi, H., Wang, T., Muhtar, W., Du, M., Zhang, B., Wu, H., Yang, L., Hu, Z., Wu, X., 2014a. Simulataneous quantification of seven hippocampal neurotransmitters in depression mice by LC-MS/MS. J. Neurosci. Methods 229, 8–14.
Huang, Q., Zhang, H., H, S., Li, S., Weng, W., Chen, J., Wang, Q., He, Y., Zhang, W., Bao, X., 2014b. A sensitive and reliable dopamine biosensor was developed based on the Au@carbon dots–chitosan composite film. Biosens. Bioelectron. 52, 277–280.
Huang, X., Xu, D., Chen, J., Liu, J., Li, Y., Song, J., Ma, X., Guo, J., 2018. Smartphone-based analytical biosensors. Analyst 143, 5339–5351.
Jesús, G., Víctor, J.R., Agustín, R.G., José, L.V., Antonio, L., 2015. Electrochemical activation of an oblique angle deposited Cu catalyst film for H_2 production. Catal. Sci. Technol. 5, 2203–2214.
Kim, Y., Bong, S., Kang, Y., Yang, Y., Mahajan, R., Kim, J., Kim, H., 2010. Electrochemical detection of dopamine in the presence of ascorbic acid using graphene modified electrodes. Biosens. Bioelectron. 25, 2366–2369.
Ku, S., Palanisamy, S., Chen, S., 2013. Highly selective dopamine electrochemical sensor based on electrochemically pretreated graphite and nafion composite modified screen printed carbon electrode. J. Colloid Interface Sci. 411, 182–186.
Lai, G., Zhang, H., Jin, C., 2007. Electrocatalysis and voltammetric determination of dopamine at a calix[4]arene crown-4 ether modified glassy carbon electrode. Electroanal 19, 496–501.
Laviolette, S., 2007. Dopamine modulation of emotional processing in cortical and subcortical neural circuits: evidence for a final common pathway in schizophrenia? Schizophr. Bull. 33, 971–981.
Liu, Q., Zhu, X., Huo, Z., He, X., Liang, Y., Xu, M., 2012. Electrochemical detection of dopamine in the presence of ascorbic acid using PVP/graphene modified electrodes. Talanta 97, 557–562.
Liu, M., Chen, Q., Lai, C., Zhang, Y., Deng, J., Li, H., Yao, S., 2013. A double signal amplification platform for ultrasensitive and simultaneous detection of ascorbic acid, dopamine, uric acid and acetaminophen based on a nanocomposite of ferrocene thiolate stabilized Fe_3O_4@Au nanoparticles with graphene sheet. Biosens. Bioelectron. 48, 75–81.
Majdi, S., Jabbari, A., Heli, H., Moosavi-Movahedi, A., 2007. Electrocatalytic oxidation of some amino acids on a nickel–curcumin complex modified glassy carbon electrode. Electrochim. Acta 52, 4622–4629.
Oh, J., Yoon, Y., Heo, J., Yu, J., Kim, H., Kim, T., 2016. Electrochemical detection of nanomolar dopamine in the presence of neurophysiological concentration of ascorbic acid and uric acid using charge-coated carbon nanotubes via facile and green preparation. Talanta 147, 453–459.
Palanisamy, S., Ku, S., Chen, S., 2013. Dopamine sensor based on a glassy carbon electrode modified with a reduced graphene oxide and palladium nanoparticles composite. Microchim Acta 180, 1037–1042.
Qi, S., Zhao, B., Tang, H., Jiang, X., 2015. Determination of ascorbic acid, dopamine, and uric acid by a novel electrochemical sensor based on pristine graphene. Electrochim. Acta 161, 395–402.
Qiu, F., Huang, Y., Hu, X., Li, B., Zhang, X., Luo, C., Li, X., Wang, M., Wu, Y., Cao, H., 2019. An ecofriendly gel polymer electrolyte based on natural lignocellulose with ultrahigh electrolyte uptake and excellent ionic conductivity for alkaline supercapacitors. ACS Appl. Energy Mater. 2, 6031–6042.
Rajkumar, C., Thirumalraj, B., Chen, S., Chen, H., 2017. A simple preparation of graphite/gelatin composite for electrochemical detection of dopamine. J. Colloid Interface Sci. 487, 149–155.
Safavi, A., Maleki, N., Moradlou, O., Tajabadi, F., 2006. Simultaneous determination of dopamine, ascorbic acid, and uric acid using carbon ionic liquid electrode. Anal. Biochem. 359, 224–229.
Shervedani, R., Bagherzadeh, M., Mozaffari, S., 2006. Determination of dopamine in the presence of high concentration of ascorbic acid by using gold cysteamine self-assembled monolayers as a nanosensor. Sensor. Actuator. B Chem. 115, 614–621.
Shiddiky, M., Torriero, A., 2011. Application of ionic liquids in electrochemical sensing systems. Biosens. Bioelectron. 26, 1775–1787.
Song, W., Chen, Y., Xu, J., Tian, D., 2010. A selective voltammetric detection for dopamine using poly (gallic acid) film modified electrode. Chin. Chem. Lett. 21, 349–352.
Suherman, A., Rasche, B., Godlewska, B., Nicholas, P., Herlihy, S., Caiger, N., Cowen, P., Compton, R., 2019. Electrochemical detection and quantification of lithium ions in authentic human saliva using $LiMn_2O_4$-modified electrodes. ACS Sens. 4, 2497–2506.
Tang, T., Chen, X., Liu, J., Bezprozvanny, I., 2007. Dopaminergic signaling and striatal neurodegeneration in huntington's disease. J. Neurosci. 27, 7899–7910.
Uzun, D., Hasdemir, E., 2017. Selective and sensitive determination of dopamine via suppressing ascorbic acid using an N-(1-H-indole-3yl) methylene thiazole-2-amine thin film-modified glassy carbon electrode. Ionics 23, 759–765.
Wang, J., Huang, X., Tang, S., Shi, G., Ma, X., Guo, J., 2018. Blood triglyceride monitoring with smartphone as electrochemical analyzer for cardiovascular disease prevention. J. Biomed. Health Inf. 23, 66–71.
Wang, J., Wang, Y., Lv, H., Hui, F., Ma, Y., Lu, S., Sha, Q., Wang, E., 2006. Studies of interaction between iron (III) and intermediates of synthetic neuromelanin by means of cyclic voltammetry of $Fe(CN)_6^{3-}$ and dopamine. J. Electroanal. Chem. 594, 59–64.
Wang, X., Yang, N., Wan, Q., Wang, X., 2007. Catalytic capability of poly(malachite green) films based electrochemical sensor for oxidation of dopamine. Sensor. Actuator. B Chem. 128, 83–90.
Wang, M., Gao, Y., Zhang, J., Zhao, J., 2015. Highly dispersed carbon nanotube in new ionic liquid-graphene oxides aqueous dispersions for ultrasensitive dopamine detection. Electrochim. Acta 155, 236–243.
Xu, D., Huang, X., Guo, J., Ma, X., 2018a. Automatic smartphone-based microfluidic biosensor system at the point of care. Biosens. Bioelectron. 110, 78–88.
Xu, G., Jarjes, Z., Desprez, V., Kilmartin, P., Travas-Sejdic, J., 2018b. Sensitive, selective, disposable electrochemical dopamine sensor based on PEDOT-modified laser scribed graphene. Biosens. Bioelectron. 107, 184–191.
Xu, J., Wang, L., Shen, Y., Yuan, K., Nie, Y., Tian, Y., Jian, X., Ma, X., Guo, J., 2018c. Family-based big medical-level data acquisition system. IEEE Trans. Biomed. Circ. Syst. 15 (4), 2321–2329.
Yang, J., Hu, Y., Li, Y., 2019. Molecularly imprinted polymer-decorated signal on-off ratiometric electrochemical sensor for selective and robust dopamine detection. Biosens. Bioelectron. 135, 224–230.
Yang, Y., Li, M., Zhu, Z., 2019. A novel electrochemical sensor based on carbon nanotubes array for selective detection of dopamine or uric acid. Talanta 201, 295–300.
Yu, D., Zeng, Y., Qi, Y., Zhou, T., Shi, G., 2012. A novel electrochemical sensor for determination of dopamine based on AuNPs@SiO_2 core-shell imprinted composite. Biosens. Bioelectron. 38, 270–277.
Yuan, D., Yuan, X., Zhou, S., Zou, W., Zhou, T., 2012. N-Doped carbon nanorods as ultrasensitive electrochemical sensors for the determination of dopamine. RSC Adv. 2, 8157–8163.
Yuan, H., Li, H., Zhang, T., Li, G., He, T., Du, T., Feng, S., 2018. A $K_2Fe_4O_7$ superionic conductor for all-solid-state potassium metal batteries. J. Mater. Chem. 6, 8413–8418.
Yusoff, N., Pandikumar, A., Ramaraj, R., Lim, H., Huang, N., 2015. Gold nanoparticle based optical and electrochemical sensing of dopamine. Microchim Acta 182, 2091–2114.
Zen, J., Hsu, C., Hsu, Y., Sue, J., Conte, E.D., 2004. Voltammetric peak separation of dopamine from uric acid in the presence of ascorbic acid at greater than ambient solution temperatures. Anal. Chem. 76, 4251–4255.
Zhang, X., Liu, S., Jiao, K., Hu, Y., 2008. Fabrication, characterization, and application of 'sandwich-type' electrode based on single-walled carbon nanotubes and room temperature ionic liquid. Electroanal 17, 1909–1916.
Zhao, D., Yu, J., Tian, K., Xu, C., 2016. A highly sensitive and stable electrochemical sensor for simultaneous detection towards ascorbic acid, dopamine, and uric acid based on the hierarchical nanoporous PtTi alloy. Biosens. Bioelectron. 82, 119–126.